Application of Wrinkling Criterion for Prediction of Side-Wall Wrinkles in Deepdrawing of Conical Cups

H. H. Wisselink[1,a], G. T. Nagy[2,b] and T. Meinders[3,c]

[1]Materials innovation institute, P.O. Box 5008, 2600GA Delft, The Netherlands
[2]Tata Steel Research, Development & Technology P.O. Box 10000, 1970CA IJmuiden, The Netherlands
[3]Faculty of Engineering Technology, University of Twente P.O. Box 217, 7500AE Enschede, The Netherlands
[a]h.wisselink@m2i.nl, [b]geza.nagy@tatasteel.com, [c]v.t.meinders@utwente.nl

Keywords: Wrinkling, Conical deep drawing, Anisotropy.

Abstract. A wrinkling indicator is used to predict the development of wrinkles in a conical cup of relatively thin packaging steel. The results of FEM simulations using a wrinkling indicator are validated with a set of experiments with varying blankholder force and lubrication.

Introduction

Due to the increasing quality of packaging steels, the wall thickness of products is generally getting smaller resulting in a reduction of the weight of the cups. Wrinkles or pleats are forming defects, resulting from (local) mechanical instability, that are to be avoided. However the risk of wrinkling during forming is increasing with decreasing thickness of the sheet. Hence, when designing or setting-up a forming facility, it is most useful to know in advance whether wrinkles will be formed and how the process settings can be changed to suppress them, without triggering other defects.

The sidewall of a drawn conical cup (Fig. 1), has an angle β. Cup designers often want a large value of this angle. However an increasing angle β leads to larger wrinkling risk in the unsupported sidewall of the cup. This study presents the use and validation of a wrinkling indicator for the prediction of sidewall wrinkles in a conical cup .

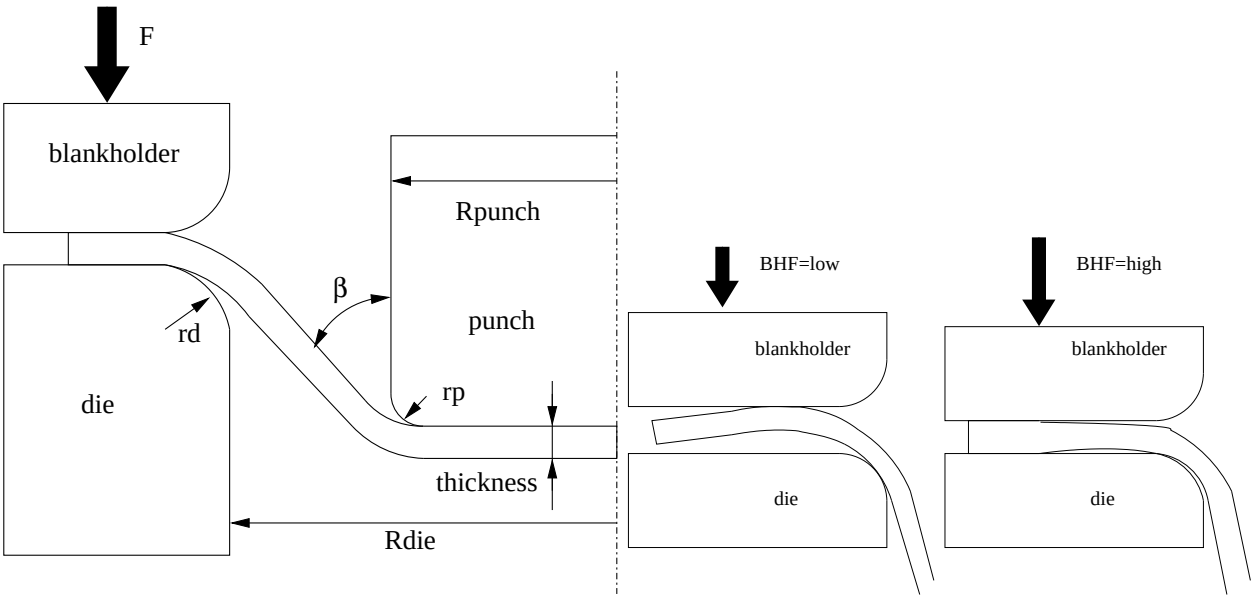

(a) Cup drawing. (b) Low force. (c) High force.

Figure 1: Schematic of conical cup drawing indicating contact cases.

Wrinkling indicator

In principle modern finite element simulations are a tool to predict wrinkling. However several studies into side-wall [1, 2] and flange wrinkling [3] show that the prediction of wrinkles is very sensitive for the chosen mesh density. Therefore to be able to detect even the slightest wrinkling tendency, for various mesh densities, a wrinkling criterion should be coupled to these simulations.

In this paper the Hutchinson-Neale wrinkling criterion [4, 5] will be used to assess the wrinkling risk. Combining the shallow shell and plastic buckling theories, equations have been derived for the onset of wrinkling in the contact free case [4]. For conical cups the assumption can be made that wrinkling is aligned with one of the principal curvature (and stress) directions. This leads to some simplifications of the general theory, which allows to derive the explicit formulas of Eq. 1 for the critical wrinkling stress σ_1^{cr} and the critical wavelength parameter λ_1^{cr} for wrinkles aligned perpendicular to the major principal stress direction [4]. A similar relation holds for σ_2^{cr} and R_1.

$$\sigma_1^{cr} = \frac{t}{\sqrt{3}R_2}\sqrt{(L_{11}L_{22} - L_{12}^2)}. \qquad \lambda_1^{cr} = \left[2\sqrt{3}\frac{\sqrt{(L_{11}L_{22} - L_{12}^2)}}{L_{11}}\right]^{\frac{1}{2}}. \tag{1}$$

These critical values depend on the sheet thickness t, the radius of curvature R in perpendicular direction and the incremental moduli of the material L_{ii} relating stress and strain. The critical wavelength is then

$$L_1^{cr} = \frac{2\pi\sqrt{R_2 t}}{\lambda_1^{cr}}. \tag{2}$$

The contact free theory has been extended to single sided contact, which leads to Eq. 3 [6]. These formulas are applicable in the flange, where the blankholder is lifted for low blankholder forces (Fig. 1b). It is expected that in true double-sided contact , which is possible under the blankholder for large blankholder forces (Fig. 1c), wrinkling will virtually not occur. Due to thickness differences the contact state will be mainly single sided contact.

$$\sigma_1^{cr} = \frac{t}{\sqrt{3}R_2}\sqrt{2L_{11}^2\left(\frac{R_2}{R_1}\right)^2 + 3L_{11}L_{22} + 4L_{11}L_{22}\left(\frac{R_2}{R_1}\right) - L_{12}^2}. \tag{3}$$

$$\lambda_1^{cr} = \left[2\sqrt{3}\frac{\sqrt{2L_{11}^2\left(\frac{R_2}{R_1}\right)^2 + 3L_{11}L_{22} + 4L_{11}L_{22}\left(\frac{R_2}{R_1}\right) - L_{12}^2}}{L_{11}}\right]^{\frac{1}{2}}. \tag{4}$$

Using the critical wrinkling stress a wrinkling indicator is defined in Eq. 5. A value above one indicates that wrinkling will occur. For negative principal stresses only, one of the formulas without or single sided contact is evaluated depending on the local contact conditions.

$$f_\sigma = \max\left(\frac{|\sigma_1|}{\sigma_1^{cr}}, \frac{|\sigma_2|}{\sigma_2^{cr}}\right). \tag{5}$$

This wrinkling indicator is determined at the end of every increment of a FEM simulation by a user subroutine as a postprocessing value. For every element the indicator is calculated on local data, the average values of element thickness and stress, and therefore very efficient.

Experiments conical cup

The presented wrinkling indicator is validated on a conical deep draw problem (Fig. 1). A set of cups of thin tinplate have been produced with increasing blankholder force, which resulted in cups

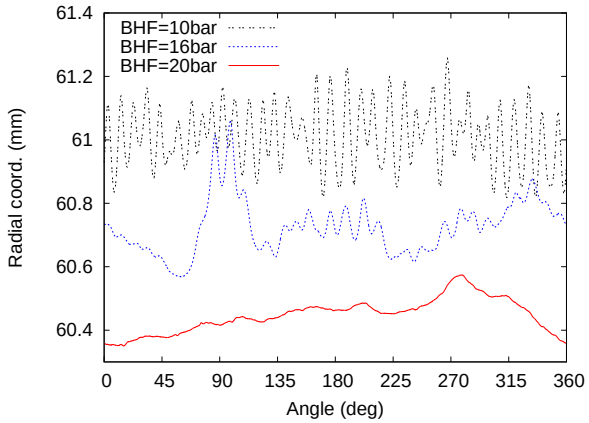

(a) Unlubricated tinplate.

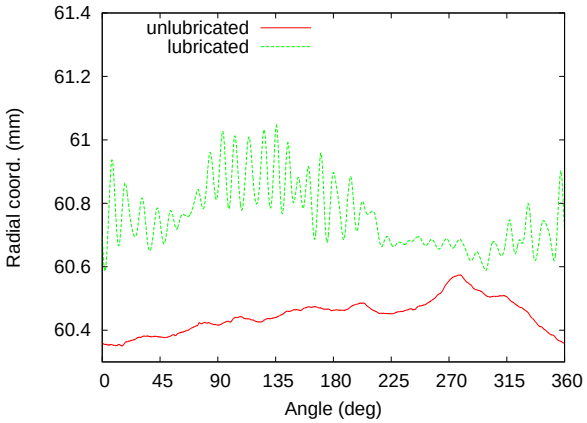

(b) BHF=20bar.

Figure 2: Measured cup side-wall profile along perimeter.

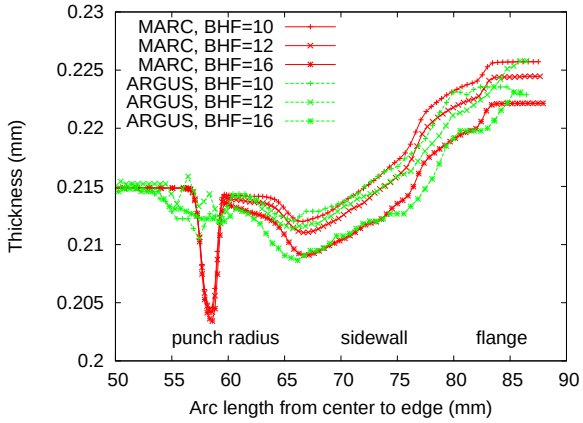

(a) Unlubricated $\mu = 0.12$.

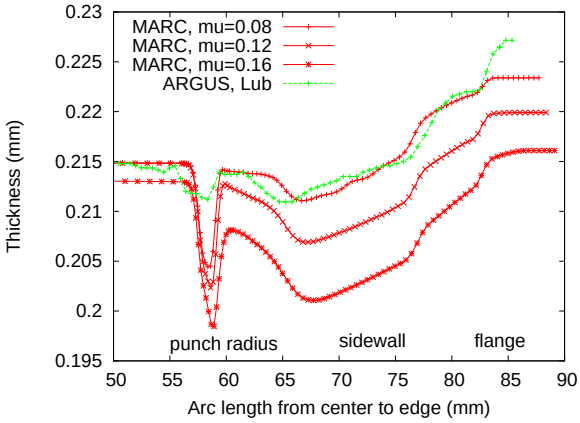

(b) Lubricated, BHF=20bar.

Figure 3: Measured and predicted cup thickness on section along RD from center.

with and without side-wall wrinkles. The blankholder force is given as the hydraulic pressure of the cylinder (BHF10 means 10 bar pressure), which is converted to the blankholder force.

The wrinkle heights obtained from the measured profile of the cup sidewall are shown in Fig. 2. It can be seen that increasing blankholder force decreases the wrinkle height (Fig. 2a), but adding lubrication increases the wrinkle height again (Fig. 2b). Although the unlubricated cup with a BHF of 20 bar is still not perfectly round it is judged as wrinkling-free. Furthermore it can be seen that the wrinkle height varies along the perimeter of the cup due to anisotropy and tool misalignment.

The optical 3D forming analysis system ARGUS has been used to measure the strains of the cups. The thickness of the final cups, which has been derived from the measured strains, is given in Fig. 3 for the Rolling Direction (RD). The thickness decreases with increasing blankholder force. The used resolution of 1 mm is too low for accurate strain measurement on the small punch radius. Direct thickness measurements show a sharp reduction of the wall thickness at the punch radius.

Simulations conical cup

The conical deepdrawing process has been simulated using MSC.Marc. A quarter of the cup has been modelled with solid shell elements (element type 185). These elements allow for through thickness stress, which needs to be included for an accurate stress prediction in areas of double sided contact under the blankholder. It proved that accounting for thickness stress has a noticeable effect on the predicted flange thickness of the cup for larger blankholder forces, which can not be modelled with

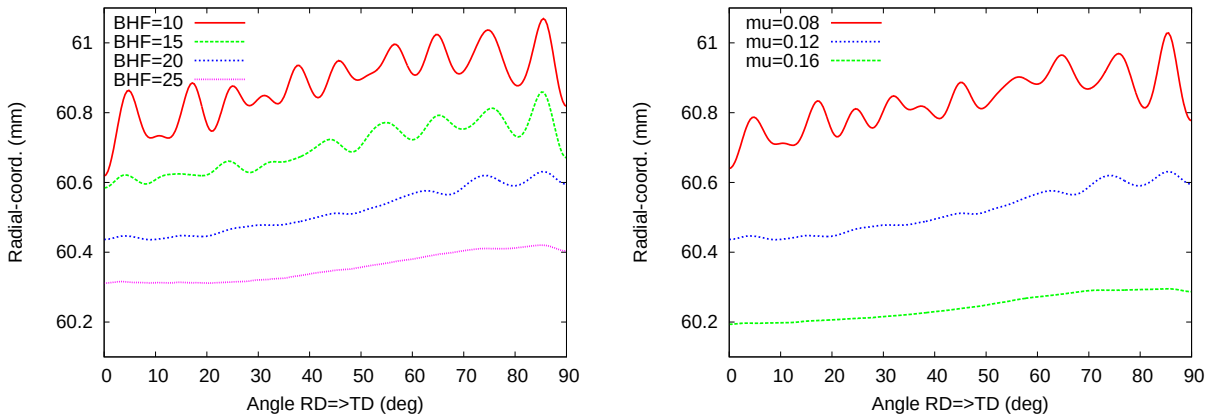

(a) Unlubricated $\mu = 0.12$.

(b) BHF=20bar.

Figure 4: Predicted cup side-wall profile halfway cup height.

common plane stress shell elements. It is assumed that the mesh is fine enough to capture wrinkles. The wrinkling criterion has been applied by Selman [7, 8] on a hemispherical cup as criterion for adaptive element refinement.

The Hill48 material model has been used to model the planar anisotropy of the 0.215 mm thick tinplate taking $r_0 = 1.65$, $r_{45} = 1.68$ and $r_{90} = 1.35$. The hardening curve is approximated with a Nadai law $\sigma_y = 527.4(0.017 + \varepsilon)^{0.194}$. The friction coefficient used in the simulations was fitted to the measured sheet thickness for the unlubricated tinplate cups. A good agreement was found for $\mu = 0.12$ as can be seen in Fig. 3. The predicted side-wall wrinkling is presented in Fig. 4. It shows a similar trend as has been measured (Fig. 2). The wrinkle amplitude decreases and the wrinkle wavelength increases with increasing blankholder force. Besides that the amount of barreling of the cup is reduced as well.

For the planar isotropic Hill yield criterion with the average Lankford-ratio r and the effective stress σ_e

$$\sigma_e = \sqrt{\sigma_1^2 - \frac{2r}{1+r}\sigma_1\sigma_2 + \sigma_2^2}. \tag{6}$$

the coefficients L_{ii} of Eq. 1 and Eq. 3 can be worked out [9].

$$\begin{aligned} L_{11} &= \frac{(1+r)^2}{1+2r}E_s - (E_s - E_t)\left(\frac{\sigma_1}{\sigma_e}\right)^2. \\ L_{22} &= \frac{(1+r)^2}{1+2r}E_s - (E_s - E_t)\left(\frac{\sigma_2}{\sigma_e}\right)^2. \\ L_{12} &= \frac{r(1+r)}{1+2r}E_s - (E_s - E_t)\left(\frac{\sigma_1\sigma_2}{\sigma_e^2}\right). \end{aligned} \tag{7}$$

The critical compressive stress in the contact free formula (Eq. 1) then becomes

$$\sigma_1^{cr} = \frac{1+r}{\sqrt{3(1+2r)}}\frac{t}{R_2}\sqrt{E_s E_t}. \qquad \sigma_2^{cr} = \frac{1+r}{\sqrt{3(1+2r)}}\frac{t}{R_1}\sqrt{E_s E_t}. \tag{8}$$

This Equation shows that wrinkling risk depends on the ratio of sheet thickness t and radius of curvature in the direction perpendicular to the principal stress. Furthermore wrinkling depends on the material anisotropy (r) and hardening law through the tangential modulus E_t and secant modulus E_s. The values of the wrinkling risk factor are presented in Fig. 5a for a cross-section halfway drawing. Critical values are predicted for the side-wall and the flange area. For conical deepdrawing the

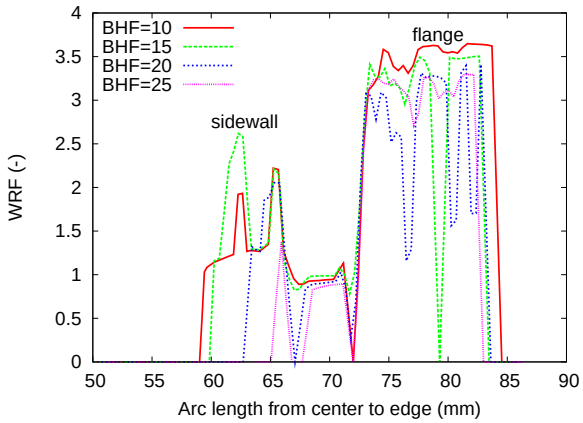

(a) Wrinkling risk factor f_σ.

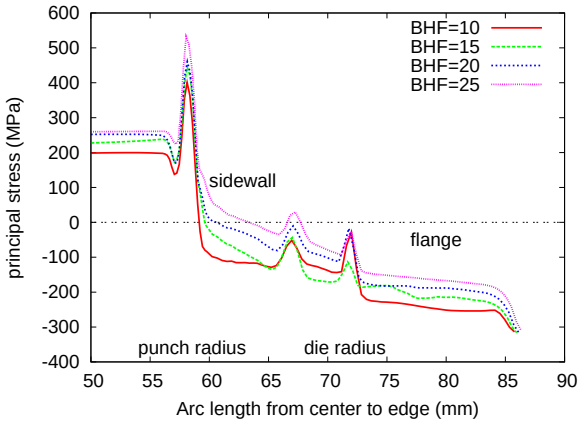

(b) Principal stress σ_2 (hoop dir.).

Figure 5: Wrinkling indicator result along RD halfway drawing.

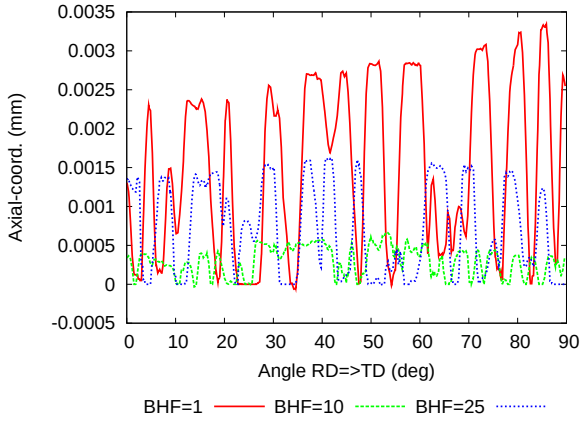

(a) Unlubricated $\mu = 0.12$.

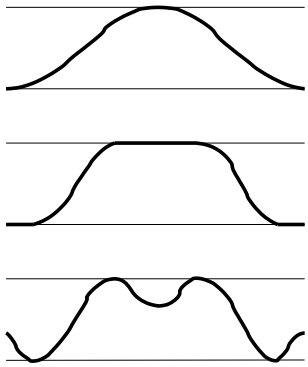

(b) Mechanism of wrinkle splitting [10].

Figure 6: Flange wrinkling at constant radius halfway drawing.

principal stress in radial direction is always positive, where the principal stress in hoop direction is negative in the side wall and flange. However for increasing blankholder force the hoop stress in the side-wall becomes positive as can be seen in Fig. 5b, which explains the decreasing wrinkling risk for increasing blankholder force. For all cases the curvatures R_1 and R_2 are almost equal.

Although small flange wrinkles have be observed in this product, these are not a problem. However the wrinkling indicator predicts high wrinkle risk in the flange and indeed flange wrinkles with very small amplitude can be detected in the simulations (Fig. 6a). Due to a small gap between the sheet and blankholder shallow wrinkles will develop, which do not grow but flatten and split into wrinkles with smaller wavelength (Fig. 6b).

For a wrinkle to develop it is not sufficient that a single element is critical, but a certain area of neighbouring elements should be critical as well. Therefore the area percentage of critical elements has been given separately for the side-wall (Fig. 7a) and flange (Fig. 7b). It can be seen that after 20% punch displacement almost 80% of the side-wall becomes critical for the lower blankholder forces. After wrinkling initiation the wrinkling indicator value drops again. The amount of critical elements in the flange does not change for the used range of blankholder forces.

Discussion and Conclusions

A wrinkling criterion has been applied for the prediction of a thin walled conical cup. It can be concluded that trends found in the experiments and simulations agree with each other. Both flange and

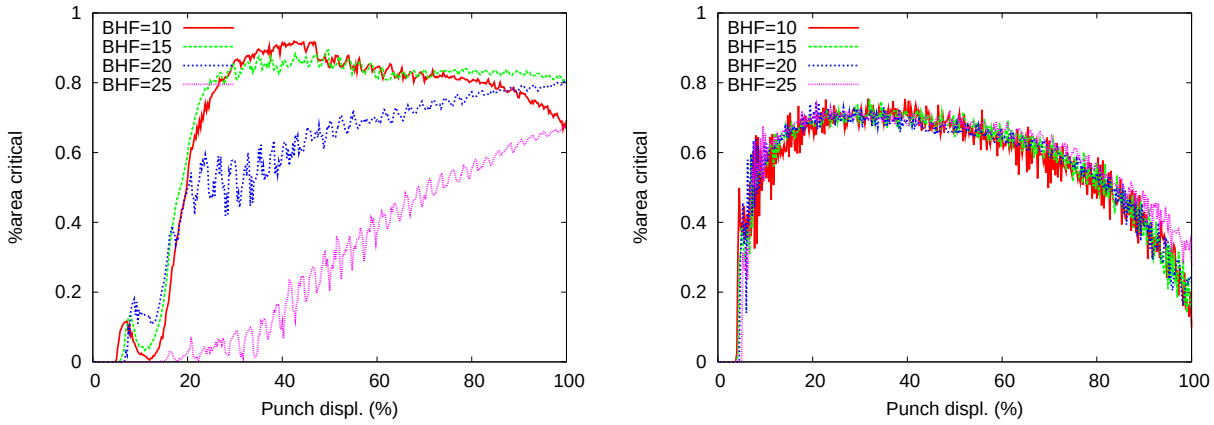

(a) Side-wall. (b) Flange.

Figure 7: Critical area during drawing.

side-wall wrinkles are present in the studied cup. Both phenomena should be separated (Fig. 7) for useful results of the wrinkling indicator. The calculated wrinkling indicator values depend strongly on the correct prediction of the hoop stress and thickness in the side-wall. These values are affected by the applied blankholder force and lubrication. Therefore these values should be known accurately for an accurate prediction of wrinkling risk.

Acknowledgements

This research was carried out under the project number MA.10205 in the framework of the Program of the Materials innovation institute M2i (www.m2i.nl).

References

[1] X. Wang and J. Cao, On the prediction of side-wall wrinkling in sheet metal forming processes, Int. J. Mech. Sci 42 (2000) 2369–2394.

[2] M. A. Shafaat, M. Abbasi, and M. Ketabchi, Investigation into wall wrinkling in deep drawing process of conical cups, J. of Materials Processing Technology 211 (2011) 1783 – 1795.

[3] J. B. Kim, J. W. Yoon, and D. Y. Yang, Investigation into the wrinkling behaviour of thin sheets in the cylindrical cup deep drawing process using bifurcation theory, Int. J. Numer. Meth. in Eng, 56 (2003) 1673–1705.

[4] J.W. Hutchinson and K.W. Neale, Wrinkling of curved thin sheet metal, In *Plastic Instability*, 1985, pp. 71–78.

[5] K.W. Neale and P.A. Tŭgcu, Numerical analysis of wrinkle formation tendencies in sheet metals, Int. J. Numer. Meth. in Eng, 30 (1990) 1595–1608.

[6] Geza T. Nagy, Kasper Valkering, and Han Huétink, Wrinkling criteria in sheet metal forming for single sided contact situation and its application, In *COMPLAS VIII*, 2005.

[7] A. Selman, Wrinkling prediction procedure in thin sheet metal forming processes with adaptive mesh refinement-part I: contact free wrinkling, Technical Report P.00.1.0016, Netherlands Institute for Metals Research, 2000.

[8] A. Selman, T. Meinders, A.H. van den Boogaard, and J. Huétink, Adaptive numerical analysis of wrinkling in sheet metal forming, Int. Journal of Forming Processes, 6 (2003) 87–102.

[9] A. Selman, E. Atzema, T. Meinders, A.H. Boogaard van den, and J. Huétink, Wrinkling in sheet metal forming: experimental testing vs. numerical analysis, Int. Journal of Forming Processes, 6 (2003) 147–160.

[10] W. Johnson and P.B. Mellor, Engineering plasticity, Van Nostrand Reinhold Co, 1973.